Extremely Active Pd@ pSiO2 Yolk–Shell Nanocatalysts for Suzuki Coupling Reactions of Aryl Halides

ARTICLE *in* THE JOURNAL OF PHYSICAL CHEMISTRY C · AUGUST 2011

Impact Factor: 4.77 · DOI: 10.1021/jp2021825

6 AUTHORS, INCLUDING:

Ji Chan Park
Korea Institute of Energy Research
51 PUBLICATIONS **1,884** CITATIONS

SEE PROFILE

Jong-Suk Kim
University of Seoul
837 PUBLICATIONS **13,044** CITATIONS

SEE PROFILE

Kang Hyun Park
Pusan National University
112 PUBLICATIONS **2,167** CITATIONS

SEE PROFILE

THE JOURNAL OF PHYSICAL CHEMISTRY C

ARTICLE

pubs.acs.org/JPCC

Extremely Active Pd@pSiO$_2$ Yolk−Shell Nanocatalysts for Suzuki Coupling Reactions of Aryl Halides

Ji Chan Park,[†] Eunjung Heo,[§] Aram Kim,[§] Mijong Kim,[‡] Kang Hyun Park,[*,§] and Hyunjoon Song[*,‡]

[†]Clean Coal Center, Korea Institute of Energy Research, Daejeon, 305-343, Korea

[‡]Department of Chemistry, Korea Advanced Institute of Science and Technology, Daejeon, 305-701, Korea

[§]Department of Chemistry and Chemistry Institute for Functional Materials, Pusan National University, Busan, Korea

Supporting Information

ABSTRACT: In the present study, we optimize the yolk−shell nanostructure in a palladium−silica system for the purpose of attaining high activity in Suzuki cross-coupling reactions. Pd@porous SiO_2 (Pd@pSiO$_2$) yolk−shell nanoparticles, bearing tiny palladium cores and highly porous silica hollow shells, were synthesized by direct silica coating and partial etching of the silica layers. High temperature treatment removed all surfactants around the catalyst surface and generated large pores on the silica shells. The resulting Pd@pSiO$_2$ yolk−shell catalysts exhibited extremely high initial turnover frequency of 78000 h^{-1}, as well as excellent reusability of more than 10 times in a standard Suzuki coupling reaction. The catalysts also catalyzed Suzuki reactions with various substrates including bromo- and chlorobenzene very well.

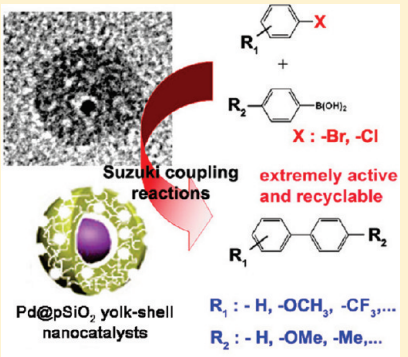

INTRODUCTION

Suzuki coupling reactions of aryl halides are very important for various applications in the chemical, pharmaceutical, and biochemical industries,[1] and on the basis of their valuable contribution, the 2010 Nobel Prize in Chemistry was awarded to Akira Suzuki jointly with Richard F. Heck and Ei-ichi Negishi for the development of palladium-catalyzed cross-coupling.[2] In this field, highly active Pd catalyst systems with enhanced reusability have been a main issue, especially for inactive substrates such as aryl chlorides.[3] For easy separation and high stability of the catalysts, ligand-free heterogeneous Pd catalysts such as Pd on activated-carbon, graphene, and metal oxide have been introduced.[4−6] However, large amounts of the catalyst and relatively long reaction times are still required to induce complete conversion of the reactants.

In common catalytic reactions, size reduction of active particles leads to a significant increase of the reactivity due to the high surface-to-volume ratio of small particles along with a large fraction of active atoms with dangling bonds exposed to the surface.[7] Prevention of particle sintering is another deterministic issue, because bare particles without any supports or stabilizers are easily agglomerated, generating large clumps that decrease their initial activity during the reaction. Such agglomeration frequently happens under harsh reaction conditions. Recently, metal@silica core−shell nanoparticles have been utilized for high temperature gas-phase reactions, resolving fundamental stability problems in a rational manner.[8−10] Metal@silica yolk−shell nanocatalysts were also introduced for various gas- and solution-phase reactions and exhibited excellent reactivity and stability at high temperatures.[11−13] These yolk−shell catalysts have outstanding structures using the entire surface of metal cores and basically hinder particle sintering by surrounding the metal cores with silica hollow shells. However, the silica shells behave as a diffusion barrier to the reactants and lower the total reaction activity. Therefore, the yolk−shell catalyst structure still needs to be optimized for maximum activity and stability in specific reactions. Reduction of the metal core size is also necessary to increase the reaction activity.[11e,14]

In the present study, we optimize the yolk−shell nanostructure in a palladium−silica system. Pd@porous SiO_2 (Pd@pSiO$_2$) yolk−shell nanoparticles, bearing tiny palladium cores and highly porous silica hollow shells, were synthesized by direct silica coating and partial etching of the silica layers in Pd@SiO$_2$ core−shell nanoparticles (Scheme 1). High temperature treatment removed all surfactants around the catalyst surface and generated large pores on the silica shells. The resulting Pd@pSiO$_2$ yolk−shell catalysts exhibited extremely high initial turnover frequency of 78000 h^{-1}, as well as excellent reusability of more than 10 times in a standard Suzuki coupling reaction. The catalysts also catalyzed Suzuki reactions with various substrates including bromo- and chlorobenzene very well.

EXPERIMENTAL SECTION

Chemicals. Palladium(II) acetylacetonate (Pd(acac)$_2$, 99%), oleylamine (Aldrich, 70%), trioctylphosphine (TOP, 90%),

Received: March 8, 2011
Revised: June 16, 2011
Published: June 16, 2011

Scheme 1. Synthetic Procedure of Pd@pSiO$_2$ Yolk−Shell Nanocatalysts

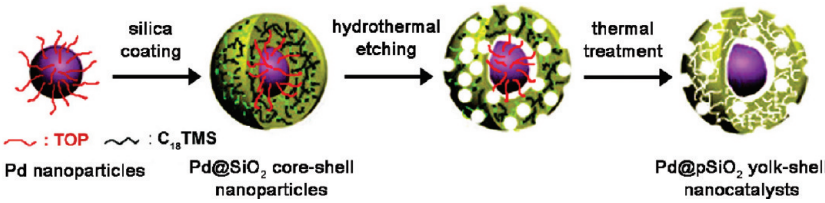

tetramethyl orthosilicate (TMOS, 98%), octadecyltrimethoxysilane (C_{18}TMS, 90%), tetraethylorthosilicate (TEOS, 98%), igepal CO-630, Pluronic P123 ($EO_{20}PO_{70}EO_{20}$), mesitylene (98%), and ammonium fluoride (NH_4F, 98+%) were purchased from Aldrich. Ammonium hydroxide (NH_4OH, 28% in water) and cyclohexane (99.5%) were purchased from Junsei. The chemicals were used as received without further purification.

Synthesis of Pd Nanoparticles. A mixture of $Pd(acac)_2$ (91 mg, 0.30 mmol), trioctylphosphine (1.0 mL, 2.25 mmol), and oleylamine (10 mL) was slowly heated from room temperature to 503 K for 20 min under an inert condition and allowed to stir at the same temperature for 40 min. After the reaction, the mixture was cooled to room temperature to yield a black suspension, and the product was precipitated by adding 50 mL of ethanol, followed by centrifugation at 10000 rpm for 20 min. The resulting Pd nanoparticles were readily dispersed in cyclohexane.

Preparation of Pd@SiO$_2$ Core−Shell Nanoparticles. Cyclohexane (25 mL) was mixed with igepal CO-630 (8.0 mL) and aqueous ammonia solution (0.80 mL), and the mixture was stirred for 20 min. The Pd particle dispersion in cyclohexane (25 mL, 6 mM with respect to the precursor concentration) was added into the mixture and allowed to stir for 30 s. TMOS (1.2 mL) and C_{18}TMS (1.2 mL) were simultaneously added into the reaction mixture, and the mixture was stirred at room temperature for 1 h. After the reaction, the product was precipitated by 30 mL of methanol, and thoroughly washed with ethanol.

Synthesis of Pd@pSiO$_2$ Yolk−Shell Catalysts. The aqueous dispersion of the Pd@SiO_2 core−shell nanoparticles (20 mL, 7.5 mM with respect to the precursor concentration) was put in a plastic bottle and placed in an oven at 383 K for 12 h. After the reaction, the product was precipitated by centrifugation at 10000 rpm for 20 min, thoroughly washed with water and ethanol, and dried in air to yield dark brown powders. The resulting Pd@pSiO$_2$ yolk−shell nanoparticles were placed at a ceramic boat in a glass tube oven, slowly heated in a ramping rate of 4 K/min from room temperature to 773 K, and aged at the same temperature for 4 h under a continuous hydrogen flow of 200 cm^3/min. After the thermal treatment, the resulting dark brown powders were cooled down to room temperature.

General Procedure for Suzuki Coupling Reactions. For the optimized reaction condition, the Pd@pSiO$_2$ yolk−shell nanocatalysts (2.0 mg, 0.28 μmol), aryl halide (1.0 mL, 9.4 mmol), phenylboronic acid (1.5 g, 12 mmol), DMF (10 mL), water (0.50 mL), and Cs_2CO_3 (6.1 g, 19 mmol) were added in a 25 mL stainless steel reactor. The mixture was stirred at 473 K for 1 h. During the reaction, the internal pressure of the reaction chamber increased to 4.2 atm. After the reaction, the Pd@pSiO$_2$ yolk−shell catalysts were separated from the clean solution by centrifugation. For recycling tests, the Pd@pSiO$_2$ yolk−shell catalysts were adsorbed on siliceous mesostructured cellular foams (MCFs). The MCFs were synthesized by the hydrothermal reaction according to the literature.[15] The reactions were carried out under the same reaction conditions. After the reaction, the catalysts with MCFs were completely separated from the clean solution by centrifugation. The resulting catalysts were used for further reactions.

Synthesis of Pd/SBA-15 Catalysts. $PdCl_2$ (0.025 g, 0.14 mmol) was dissolved in distilled water (5.0 mL), and the solution was impregnated on SBA-15 (1.0 g) by the incipient wetness method, according to the literature.[16] The resulting sample was dried in an oven at 373 K for 1 h and reduced in a hydrogen flow of 200 cm^3/min at 773 K for 4 h.

Poisoning Test. Poly(4-vinylpyridine) (300 equiv with respect to the total Pd content) was introduced either prior to initiation of the reactions by the addition of base or during the reaction sequence.

Characterization. The nanoparticle structures were characterized by transmission electron microscopy (TEM) and high-resolution transmission electron microscopy (HRTEM) (Philips F20 Tecnai operated at 200 kV, KAIST). Samples were prepared by putting a few drops of the corresponding colloidal solutions on carbon-coated copper grids (Ted Pellar, Inc.). X-ray powder diffraction (XRD) patterns were recorded on a Rigaku D/MAX-RB(12 kW) diffractometer. The palladium loading amounts were measured by inductively coupled plasma atomic emission spectrometry (ICP-AES) (POLY SCAN 60 E). The CO adsorption was measured by BELSORP-HP (BEL Japan Inc.) at 298 K, and nitrogen sorption isotherms were measured at 77 K with a BELSORP mini-II (BEL Japan Inc.). Before the N_2 sorption measurements, the samples were degassed in a vacuum at 623 K for 6 h. The coupling reaction products were analyzed by ^{1}H NMR using Varian Mercury Plus (300 MHz). Chemical shift values were recorded as parts per million relative to tetramethylsilane as an internal standard unless otherwise indicated, and coupling constants are in hertz.

RESULTS AND DISCUSSION

The Pd nanoparticles were prepared by thermal decomposition of Pd−surfactant complexes.[17] A palladium precursor, palladium(II) acetylacetonate, and trioctylphosphine (TOP) were mixed in oleylamine. The mixture was slowly heated to 503 K for 20 min and aged for an additional 40 min at the same temperature. The resulting Pd nanoparticles were washed and redispersed in cyclohexane. The TEM image indicates uniformly spherical Pd particles with an average diameter of 3.4 ± 0.2 nm (Figure 1a). The HRTEM) image shows atomic lattice fringes with a distance between adjacent fringe images of 0.225 nm, which matches with that of (111) planes in face-centered cubic (fcc) Pd (Figure 1b).

The Pd nanoparticles were successfully coated with silica by a water-in-oil microemulsion method.[18] The Pd particle

dx.doi.org/10.1021/jp2021825 |J. Phys. Chem. C 2011, 115, 15772–15777

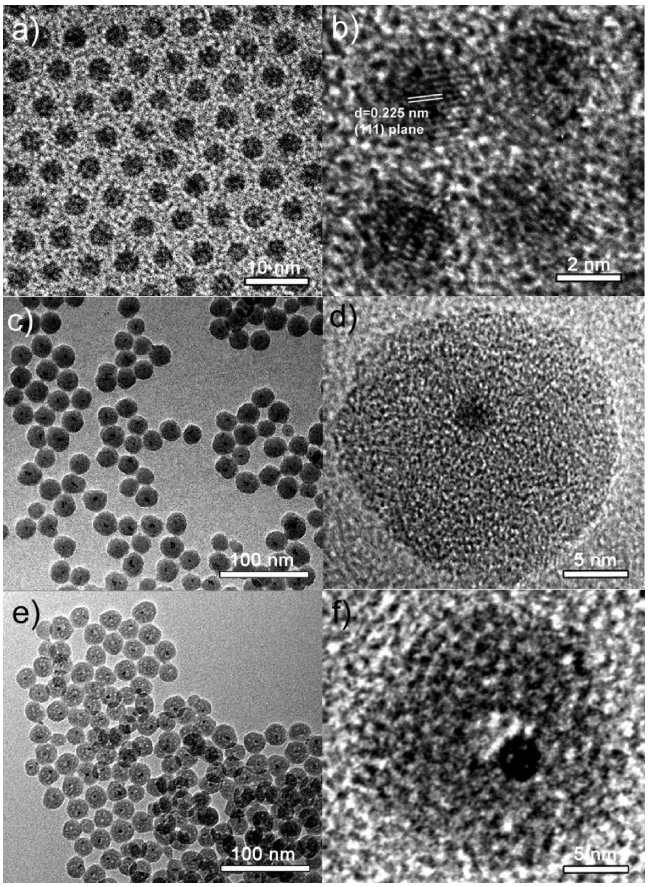

Figure 1. TEM and HRTEM images of (a, b) Pd nanoparticles, (c, d) Pd@SiO_2 core−shell nanoparticles, and (e, f) Pd@pSiO_2 yolk−shell nanoparticles.

dispersion was mixed with igepal CO-630 and ammonia, and tetramethyl orthosilicate (TMOS) and octadecyl trimethoxysiliane (C_{18}TMS) were added to the mixture. The reaction mixture was stirred at room temperature for 1 h. It is known that long chain alkyl siloxanes such as C_{18}TMS can generate irregular pores inside a silica matrix after high-temperature calcination.[19] The igepal CO-630 forms microemulsion, and ammonia catalyzes decomposition of the silica precursor during the reaction. After the reaction, more than 90% of the individual Pd particles were successfully coated with silica shells. The average thickness of the silica shells was measured to be 9.7 ± 1.5 nm (Figure 1c,d). Hollowing silica shells were conducted by partial dissolution of the silica under a benign basic solution.[20] The Pd@SiO_2 core−shell nanoparticles were dispersed in distilled water and aged under hydrothermal conditions for 12 h. The resulting silica layers were less dense and had multiple large pores that could be identified in the TEM images. Interestingly, the silica component that is in direct contact with the Pd core surface was nearly removed, leading to the formation of a yolk−shell type structure (Figure 1e,f). The particles are referred to as Pd@pSiO_2 yolk−shell nanoparticles, because the silica shell layers are highly porous.

In order to remove all organic residues such as C_{18}TMS and surfactants, the Pd@pSiO_2 yolk−shell nanoparticles were heated at 773 K under a hydrogen flow for 4 h. After the thermal treatment, the average core size was measured to be 3.5 ± 0.3 nm (Figure 2a); this value is identical to that of the thermally

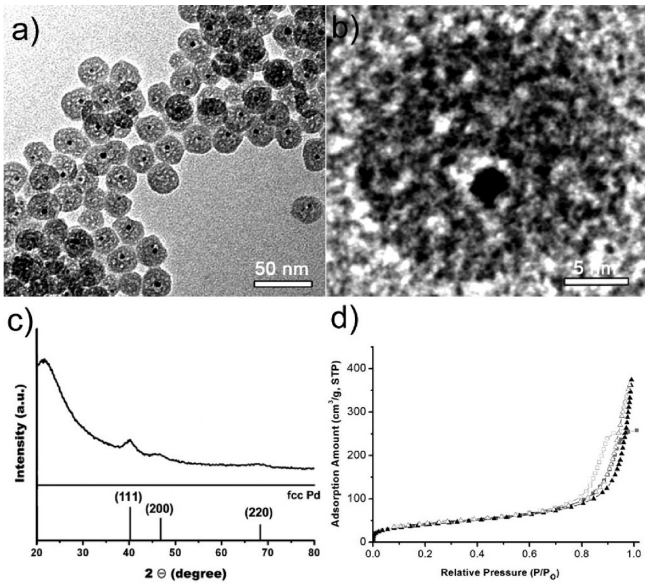

Figure 2. (a, b) TEM images and (c) XRD pattern of Pd@pSiO_2 yolk−shell nanocatalysts after thermal treatment. (d) N_2 adsorption−desorption isotherms of Pd@SiO_2 core−shell nanoparticles (■, □) and Pd@pSiO_2 yolk−shell nanocatalysts (▲, Δ) after thermal treatment.

untreated structure, indicating high thermal stability of the tiny Pd cores surrounded by the silica hollow shells. The TEM image of a single particle clearly shows a bright region around the Pd core in the silica shell, which confirms the yolk−shell type structure (Figure 2b). The XRD pattern of the Pd@pSiO_2 yolk−shell nanoparticles matches with that of face-centered cubic (fcc) Pd (Figure 2c, JCPDS No. 46-1043). The Pd particle size calculated from line broadening of the (111) reflection by the Debye−Scherrer equation is 3.6 nm, in good agreement with that from the TEM images. A N_2 sorption experiment at 77 K for the particles exhibits a type IV adsorption−desorption with type H3 hysteresis, and the BET (Brunauer−Emmett−Teller) surface area is calculated to be 145 $m^2\ g^{-1}$ (Figure 2d). The total pore volume of the yolk−shell particles is 0.57 $cm^3\ g^{-1}$, which is 40% higher than that (0.40 $cm^3\ g^{-1}$) of the core−shell particles. These values also verify effective pore generation during the partial silica etching step. The Pd loading content of the yolk−shell nanoparticles is measured to be 1.5 wt % by ICP-AES. A total surface area of the Pd cores is estimated to be 179 $m^2\ g^{-1}$, by CO gas adsorption in fresh Pd@SiO_2 yolk−shell nanoparticles after hydrogen treatment at 673 K. The average core size is calculated to be 2.8 nm, comparable to the real Pd core size measured by the TEM and XRD data. It indicates that the surfactants and carbon residues are completely removed by thermal treatment, and thus the active surface of the Pd cores is fully accessible by incoming reagents.

The Pd@pSiO_2 yolk−shell nanocatalysts were employed for Suzuki coupling reactions of bromobenzene with phenylboronic acid. Under common conditions at room temperature, the conversion approaches 100% for a reaction time of 6 h in the presence of 0.1 mol % Pd catalysts (entry 1, Table 1). The yolk−shell nanocatalysts have a notable advantage of high temperature stability,[11,12] and thus the solvent and reaction temperature were adjusted to maximize reaction activity (Table 1). The reactions were screened with variable catalyst

Table 1. Suzuki Coupling Reactions of Bromobenzene with Phenylboronic Acid

entry	Pd (mol %)	T (K)	t (h)	base	conv (%)[a]
1	0.1	298	6	K_2CO_3	100
2	0.005	473	3	K_2CO_3	100
3[b]	0.003	523	1	K_2CO_3	17
4	0.003	473	1	Na_2CO_3	71
5	0.003	473	1	Cs_2CO_3	100
6	0.003	473	0.50	Cs_2CO_3	45 (30)
7	0.003	473	0.17	Cs_2CO_3	39 (23)
8[c]	0.003	473	1	Cs_2CO_3	35
9[d]	0.003	473	1	Cs_2CO_3	72
10[e]	0.003	473	1	Cs_2CO_3	40
11	0.002	473	1	Cs_2CO_3	63

[a] Determined by ^{1}H NMR spectra. [b] NMP/H_2O (20:1) as a solvent mixture. [c] Free-standing Pd nanoparticles. [d] Pd@pSiO_2 yolk−shell nanoparticles before thermal treatment. [e] Pd@SiO_2 core−shell nanoparticles. The values inside the parentheses are isolated yields of the product.

amounts and reaction temperatures (entries 2−4, Table 1, and all entries in Table S1, Supporting Information). It was found that the optimal conditions of the reaction were utilizing a mixture of DMF (dimethylformamide) and water as reaction media and Cs_2CO_3 as a base, in the presence of 0.003 mol % (2.0 mg, 0.28 μmol) of the catalyst at 473 K (entry 5, Table 1). Under this reaction condition, the reactions were carried out for 1, 0.5, and 0.17 h, and the yields were 100, 45, and 39%, respectively (entries 5−7). The isolated yields of the products were a little less than the conversions measured by ^{1}H NMR, mainly because of a loss during the workup process. Remarkably, the average turnover frequency (TOF) for 1 h (entry 5) is 33000 h^{-1}, calculated by the moles of bromobenzene consumed per moles of the palladium catalyst per 1 h under the present conditions. The initial TOF value approaches 78000 h^{-1} at the early reaction period up to 10 min (entry 7). Although the supported Pd nanocatalysts such as Pd/SBA-15 and Pd/C nanostructures have shown good activities under the specific reaction conditions,[21] the Pd@pSiO_2 yolk−shell nanocatalyst would be one of the best catalysts for Suzuki coupling reactions, in terms of small usage for complete conversion, extremely high activity, and excellent endurance at high temperature. It is noted that the general Suzuki coupling reactions use 0.1−0.01 mol % of Pd catalysts with respect to the amount of the substrate for complete conversion.

In order to verify the factors that lead to such high reactivity in this yolk−shell nanocatalyst structure, control experiments were designed with different catalysts including free-standing Pd nanoparticles, Pd@SiO_2 core−shell nanoparticles, and Pd@pSiO_2 yolk−shell nanoparticles prior to thermal treatment under identical reaction conditions (entries 8−10, Table 1). The order of the conversion yield is: Pd@pSiO_2 yolk−shell nanocatalysts (100%) > Pd@pSiO_2 yolk−shell nanoparticles before thermal treatment (72%) > Pd@SiO_2 core−shell nanoparticles (40%) > free-standing Pd nanoparticles (35%). The Pd@pSiO_2 yolk−shell catalysts are substantially more active than the Pd@SiO_2 core−shell particles, due to the completely exposed surface of the Pd cores and fast diffusion of the reactants through the porous silica layers (entries 5 and 10, Table 1). Thermal treatment can effectively generate large pores and a clean metal surface, which lead to high conversion of the reactants compared

Table 2. Suzuki Coupling Reactions of Various Aryl Halides with Arylboronic Acids Catalyzed by Pd@pSiO_2 Yolk−Shell Nanocatalysts[a]

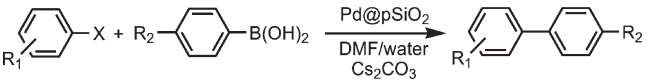

entry	R_1	R_2	X	t (h)	yield (%)[b]
1	H	H	Cl	3	100
2	4-OCH_3	H	Br	3	64
3	4-CHO	H	Br	3	64
4	2-CHO	H	Br	3	100
5	4-CF_3	H	Br	3	61
6	4-CHO	H	Cl	3	68
7	2-CHO	H	Cl	3	100
8	H	OMe	Br	3	100
9	H	Me	Br	3	87

[a] Reaction conditions: aryl halide, arylboronic acid, Pd@pSiO_2 yolk−shell nanocatalysts (0.003 mol % with respect to aryl halide concentration), Cs_2CO_3 (2.0 equiv), DMF/water (20:1) at 473 K. [b] Isolated yield.

to the case of untreated particles (entries 5 and 9, Table 1). The free-standing Pd nanoparticles exhibit the lowest activity (entry 8, Table 1), which is mainly attributed to the reduction of active surface area in the particles during the reaction, owing to severe particle agglomeration, as shown in the TEM image (Figure S1, Supporting Information). For the comparison with common Pd/SiO_2 catalysts, the Pd/SBA-15 catalyst with the Pd loading content of 1.5% was synthesized through the incipient wetness method.[16] The TEM image of the catalyst shows that the palladium particles were actually formed on the SBA-15 channels. The XRD spectrum has three peaks assignable to fcc Pd (JCPDS #46-1043), indicating the Pd(0) nanoparticle formation (Figure S2, Supporting Information). The Pd/SBA-15 catalyst was directly utilized for the reaction under the optimized condition as used in entry 5 and exhibited the conversion yield of 67%, lower than the complete conversion of the Pd@pSiO_2 yolk−shell catalyst. It may result from the formation of large Pd particles under the synthetic conditions and bad stability of the particles during the high temperature reactions.

The optimized reaction conditions with the Pd@pSiO_2 yolk−shell catalysts were applied to various substituents (Table 2). One of the main issues in Suzuki coupling reactions is activating aryl chlorides, which generally show low conversion yields under normal reaction conditions. The Pd@pSiO_2 yolk−shell catalysts lead to complete conversion of chlorobenzene with phenylboronic acid within 3 h (entry 1, Table 2). The study was extended by substituting electron-donating or -withdrawing groups on both bromobenzenes and chlorobenzenes. Generally, a favorable effect of electron-withdrawing substituents is observed in palladium catalyzed reactions.[22] However, in our catalytic system, both bromobenzenes and chlorobenzenes, including either electron-withdrawing substituents such as CHO and CF_3 or electron-donating substituents such as OCH_3, are readily coupled with arylboronic acids in good yields (entries 2−7, Table 2). High reactivity with an excellent yield is also observed in the couplings of *o*-bromobenzaldehyde or *o*-chlorobenzaldehyde with phenylboronic acid, which produces corresponding biaryls (entries 4 and 7, Table 2). Furthermore, a

variety of substituted arylboronic acids are successfully coupled with 4-bromobenzene. The coupled products are obtained in high yields, when 4-bromobenzene reacts with any of the electron-rich 4-methoxy or 4-methylphenylboronic acid (entries 8−9, Table 2). For easy recovery, the Pd@pSiO$_2$ yolk−shell nanocatalysts were diluted with MCFs (siliceous mesostructured cellular foams)[15] to reduce a possible loss during the separation procedure. The resulting catalysts exhibit high recyclability with a substrate/Pd molar ratio of 1000:1. The initial activity is completely maintained for more than 10 cycles.

There have been many studies on the interaction of Pd catalysts with substrates and intermediates in Suzuki coupling reactions.[23] The reactions can proceed in a heterogeneous manner on the surface of solid Pd, or via a quasi-homogeneous mechanism, where Pd is dissolved as colloids or as organometallic complexes by oxidative addition to the substrates.[24] In our catalytic system, the Pd@pSiO$_2$ yolk−shell catalysts appear to catalyze the coupling reactions in a heterogeneous manner. The coupling reaction in the presence of poly(4-vinylpyridine), which behaves as a poison to trap homogeneous Pd species through chelation in the solution phase, shows no obvious change in catalytic activity. Furthermore, no coupling reaction is carried out after the catalyst removal by microfiltration, demonstrating the absence of dissolved Pd species in the reaction mixture.

CONCLUSION

In summary, we optimized the yolk−shell nanostructure for the purpose of attaining high activity in Suzuki cross-coupling reactions. The Pd@pSiO$_2$ yolk−shell nanocatalysts comprise tiny Pd cores with fully accessible surfaces, as well as highly porous silica hollow shells that do not significantly limit diffusion rates of the substrates. The surfactants are completely removed by prolonged thermal treatment. Owing to this rational design and synthesis, the resulting Pd@pSiO$_2$ yolk−shell catalysts exhibit extremely high activities for Suzuki coupling reactions of various bromo- and chlorobenzene substituents with arylboronic acid and show good recyclability. While there have been many notable achievements in the field of nanocatalysts with well-defined morphology thus far, the reaction results could not complete with those of commercial catalysts.[25] Our yolk−shell catalyst system has distinct advantages of high thermal stability and recyclability, and in this experiment, extremely high activity was also achieved in industrially valuable C−C coupling reactions. It is anticipated that the range of application of such rationally designed nanostructured catalysts can be continuously expanded to various gas- and solution-phase reactions, and the catalysts will satisfy all requirements necessary for actual industrial uses.

ASSOCIATED CONTENT

Supporting Information. TEM images and experimental data of Pd/SBA-15 and free-standing nanoparticles after the reaction and Suzuki coupling reactions of bromobenzene and phenylboronic acid catalyzed by Pd@pSiO$_2$ yolk−shell nanocatalysts under various conditions. This material is available free of charge via the Internet at http://pubs.acs.org.

AUTHOR INFORMATION

Corresponding Author

*E-mail: chemistry@pusan.ac.kr, hsong@kaist.ac.kr.

ACKNOWLEDGMENT

This work was supported by the Core Research Program (2010-07592) and the Basic Science Research Program (2009-0070926, 2010-0002834) through the National Research Foundation of Korea (NRF) funded by the Ministry of Education, Science and Technology. J.C.P. thanks to the Korea Student Aid Foundation (KOSAF) grant funded by the Korean government (MEST) (No. S2-2009-000-00951-1).

REFERENCES

(1) Miyaura, N.; Suzuki, A. *Chem. Rev.* **1995**, *95*, 2457–2483.

(2) See: http://nobelprize.org/nobel_prizes/chemistry/laureates/2010/.

(3) (a) Choi, M.; Lee, D.-H.; Na, K.; Yu, B.-W.; Ryoo, R. *Angew. Chem., Int. Ed.* **2009**, *48*, 3673–3676. (b) Jin, M.-J.; Lee, D.-H. *Angew. Chem., Int. Ed.* **2010**, *49*, 1119–1122.

(4) (a) Kitamura, Y.; Sako, S.; Udzu, T.; Tsutsui, A.; Maegawa, T.; Monguchi, Y.; Sajiki, H. *Chem. Commun.* **2007**, 5069–5071. (b) Maegawa, T.; Kitamura, Y.; Sako, S.; Udzu, T.; Sakurai, A.; Tanaka, A.; Kobayashi, Y.; Endo, K.; Bora, U.; Kurita, T.; Kozaki, A.; Monguchi, Y.; Sajiki, H. *Chem.—Eur. J.* **2007**, *13*, 5937–5943.

(5) Scheuermann, G. M.; Rumi, L.; Steurer, P.; Bannwarth, W.; Mülhaupt, R. *J. Am. Chem. Soc.* **2009**, *131*, 8262–8270.

(6) (a) Erathodiyil, N.; Ooi, S.; Seayad, A. M.; Han, Y.; Lee, S. S.; Ying, J. Y. *Chem.—Eur. J.* **2008**, *14*, 3118–3125. (b) Webb, J. D.; MacQuarrie, S.; McEleney, K.; Crudden, C. M. *J. Catal.* **2007**, *252*, 97–109.

(7) Goesmann, H.; Feldmann, C. *Angew. Chem., Int. Ed.* **2010**, *49*, 1362–1395.

(8) Joo, S. H.; Park, J. Y.; Tsung, C.-K.; Yamada, Y.; Yang, P.; Somorjai, G. A. *Nat. Mater.* **2009**, *8*, 126–131.

(9) (a) Tago, T.; Shibata, Y.; Hatsuta, T.; Miyajima, K.; Kishida, M.; Tashiro, S.; Wakabayashi, K. *J. Mater. Sci.* **2002**, *37*, 977–982. (b) Montini, T.; Condo, A. M.; Hickey, N.; Lovey, F. C.; De Rogatis, L.; Fornasiero, P.; Graziani, M. *Appl. Catal., B* **2007**, *73*, 84–97. (c) Specchia, S.; Vella, L. D.; Lorenzut, B.; Montini, T.; Specchia, V.; Fornasiero, P. *Ind. Eng. Chem. Res.* **2010**, *49*, 1010–1017.

(10) (a) Gombac, V.; Sordelli, L.; Montini, T.; Delgado, J. J.; Adamski, A.; Adami, G.; Cargnello, M.; Bernal, S.; Fornasiero, P. *J. Phys. Chem. A* **2010**, *114*, 3916–3925. (b) Montini, T.; De Rogatis, L.; Gombac, V.; Fornasiero, P.; Graziani, M. *Appl. Catal., B* **2007**, *71*, 125–134.

(11) (a) Park, J. C.; Song, H. *Nano Res.* **2011**, *4*, 33–49. (b) Lee, J.; Park, J. C.; Song, H. *Adv. Mater.* **2008**, *20*, 1523–1528. (c) Lee, J.; Park, J. C.; Bang, J. U. *Chem. Mater.* **2008**, *20*, 5839–5844. (d) Park, J. C.; Bang, J. U.; Ko, C. H.; Song, H. *J. Mater. Chem.* **2010**, *20*, 1239–1246. (e) Park, J. C.; Lee, H. J.; Kim, J. Y.; Park, K. H.; Song, H. *J. Phys. Chem. C* **2010**, *114*, 6381–6388.

(12) (a) Arnal, P. M.; Comotti, M.; Schüth, F. *Angew. Chem., Int. Ed.* **2006**, *45*, 8224–8227. (b) Huang, X.; Guo, C.; Zuo, J.; Zheng, N.; Stucky, G. D. *Small* **2009**, *5*, 361–365.

(13) (a) Harada, T.; Ikeda, S.; Ng, Y. H.; Sakata, T.; Mori, H.; Torimoto, T.; Matsumura, M. *Adv. Funct. Mater.* **2008**, *18*, 2190–2196. (b) Ng, Y. H.; Ikeda, S.; Harada, T.; Park, S.; Sakata, T.; Mori, H.; Matsumura, M. *Chem. Mater.* **2008**, *20*, 1154–1160.

(14) (a) Valden, M.; Lai, X.; Goodman, D. W. *Science* **1998**, *281*, 1647–1650. (b) Lopez, N.; Janssens, T. V. W.; Clausen, B. S.; Xu, Y.; Mavrikakis, M.; Bligaard, T.; Nørskov, J. K. *J. Catal.* **2004**, *223*, 232–235. (c) Haruta, M. *Catal. Today* **1997**, *36*, 153–166.

(15) Schmidt-Winkel, P.; Lukens, W. W.; Yang, P., Jr.; Margolese, D. I.; Lettow, J. S.; Ying, J. Y.; Stucky, G. D. *Chem. Mater.* **2000**, *12*, 686–696.

(16) Bendahou, K.; Cherif, L.; Siffert, S.; Tidahy, H. L.; Benaissa, H.; Aboukais, A. *Appl. Catal., A* **2008**, *351*, 82–87.

(17) Son, S. U.; Jang, Y.; Yoon, K. Y.; Kang, E.; Hyeon, T. *Nano Lett.* **2004**, *4*, 1147–1151.

(18) Han, Y.; Jiang, J.; Lee, S. S.; Ying, J. Y. *Langmuir* **2008**, *24*, 5842–5848.
(19) (a) Kim, J. Y.; Yoon, S. B.; Yu, J.-S. *Chem. Commun.* **2003**, 790–791. (b) Yano, K.; Fukushima, Y. *J. Mater. Chem.* **2004**, *14*, 1579–1584.
(20) (a) Park, S.-J.; Kim, Y.-J.; Park, S.-J. *Langmuir* **2008**, *24*, 12134–12137. (b) Zhang, F.; Yan, Y.; Yang, H.; Yu, C.; Tu, B.; Zhao, D. *J. Phys. Chem. B* **2005**, *109*, 8723–8732.
(21) Yin, L.; Liebscher, J. *Chem. Rev.* **2007**, *107*, 133–173 and references therein.
(22) Barder, T. E.; Walker, S. D.; Martinelli, J. R.; Buchwald, S. L. *J. Am. Chem. Soc.* **2005**, *127*, 4685–4696.
(23) Gaikwad, A. V.; Holuigue, A.; Thathagar, M. B.; ten Elshof, J. E.; Rothenberg, G. *Chem.—Eur. J.* **2007**, *13*, 6908–6913.
(24) (a) Narayanan, R.; El-Sayed, M. A. *J. Am. Chem. Soc.* **2003**, *125*, 8340–8347. (b) Ellis, P. J.; Fairlamb, I. J. S.; Hackett, S. F. J.; Wilson, K.; Lee, A. F. *Angew. Chem., Int. Ed.* **2010**, *49*, 1820–1824.
(25) (a) Li, Y.; Boone, E.; El-Sayed, M. A. *Langmuir* **2002**, *18*, 4921–4925. (b) Narayanan, R.; El-Sayed, M. A. *Langmuir* **2005**, *21*, 2027–2033. (c) Chen, Y.-H.; Hung, H.-H.; Huang, M. H. *J. Am. Chem. Soc.* **2009**, *131*, 9114–9121.